

Transcriptome Analysis of *Myzus persicae* to UV-B Stress

Chang-Li Yang,¹ Jian-Yu Meng,² Meng-Shuang Yao,¹ and Chang-Yu Zhang^{1,3,*}

¹Institute of Entomology, Guizhou Provincial Key Laboratory for Agricultural Pest Management of the Mountainous Region, Guizhou University, Guiyang, Guizhou 550025, People's Republic of China, ²Guizhou Tobacco Science Research Institute, Guiyang, Guizhou 550081, People's Republic of China, and ³Corresponding author, e-mail: zcy1121@aliyun.com

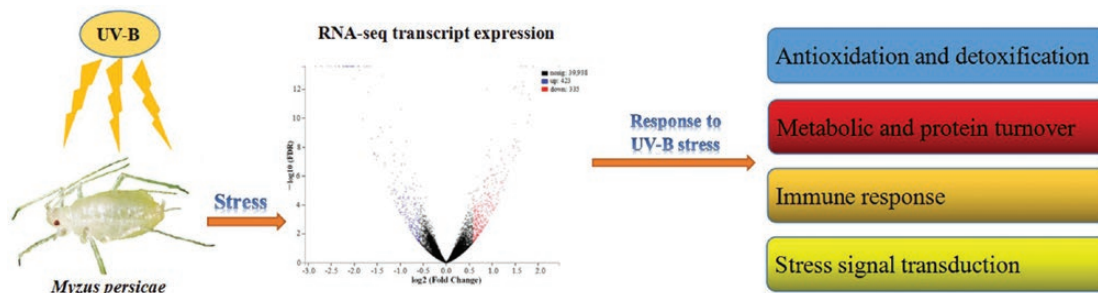
Subject Editor: Bill Bendena

Received 3 March 2021; Editorial decision 22 April 2021

Abstract

As an environmental stress factor, ultraviolet-B (UV-B) radiation directly affects the growth and development of *Myzus persicae* (Sulzer) (Homoptera: Aphididae). How *M. persicae* responds to UV-B stress and the molecular mechanisms underlying this adaptation remain unknown. Here, we analyzed transcriptome data for *M. persicae* following exposure to UV-B radiation for 30 min. We identified 758 significant differentially expressed genes (DEGs) following exposure to UV-B stress, including 423 upregulated and 335 downregulated genes. In addition, enrichment analysis using the Gene Ontology and Kyoto Encyclopedia of Genes and Genomes databases illustrated that these DEGs are associated with antioxidation and detoxification, metabolic and protein turnover, immune response, and stress signal transduction. Simultaneously, these DEGs are closely related to the adaptability to UV-B stress. Our research can raise awareness of the mechanisms of insect responses to UV-B stress.

Graphical Abstract



Key words: *Myzus persicae*, UV-B stress, transcriptome, RNA sequencing, antioxidant mechanism

Sunlight is a key environmental factor in almost all ecosystems on the planet, and the ultraviolet (UV) light of the spectrum affects both living organisms and nonliving matter in the ecosystem. It can be divided into three types according to different wavelengths: long-wave UV light (UV-A, 315–400 nm), medium-wave UV light (UV-B, 280–315 nm), and short-wave UV light (UV-C, 200–280 nm) (Paul and Gwynn-Jones 2003). The ozone layer in the Earth's atmosphere can effectively absorb most of the UV-B, but there are still 10% of which could reach the ground (Rünger and Kappes 2008). In recent years, the destruction of the stratospheric ozone layer in the Earth's atmosphere due to environmental pollution has caused a sharp increase in the amount of solar ultraviolet radiation reaching

the surface of the Earth, especially UV-B radiation (McKenzie et al. 2007). High doses of UV-B radiation are harmful to living organisms. It induces oxidative stress in living organisms by generating reactive oxygen species, leading to the destruction of DNA, membrane lipids, and proteins, which seriously affects growth, physiology, biochemistry, and population structure (Lidon et al. 2012, Hideg et al. 2013, Guo et al. 2019).

Insects are the most diverse animals; most of them live on the earth in direct sunlight (Bode et al. 2009). The development, survival, and reproduction of insects are closely related to UV-B exposure. Previous studies have reported that UV-B radiation affects the growth of *Manduca sexta* larvae (Potter and Woods 2013).

UV-B can induce the body weight and fat body index of *Osmia bicornis* decrease, with the increase of the radiation intensity, the morphological deformity of wings and mouthparts, and programmed death of germ cells in insects (Wasielewski et al. 2015). UV-B radiation increased the metabolic rate of *Aedes albopictus* and *Culex pipiens* larvae, and their survival rate was significantly reduced (Villena et al. 2018). UV-B radiation not only caused death of *Tribolium castaneum* larvae, but also delayed larval-pupal metamorphosis and reduced the size and emergence rate of pupae (Sang et al. 2016). Although UV-B is harmful to most organisms, but most insects have a complete anti-stress mechanisms, including photoprotective pigments, antioxidants, apoptosis, DNA repair, and effective mechanisms, so as to reduce the damage of UV-B to the body (Paul and Gwynn-Jones 2003, Dahms and Lee 2010, Vandebussche et al. 2018, Villena et al. 2018). Under UV-B radiation, brown form is more tolerant than green form in *Sitobion avenae*, and its nymph development period is shorter and the total fecundity is higher (Hu et al. 2013). In addition, the activities of superoxide dismutase (SOD), peroxidase (POD), and catalase are higher in *Spodoptera litura* under UV-B radiation (Karthi et al. 2014). However, there are few studies on systematically describing the overall physiological response of insects in response to UV-B radiation. Transcriptome is a high-throughput sequencing of mRNA from a species, and the results reflect the expression level of the entire genome of the species under specific conditions and at specific time points (Croucher et al. 2009). It is widely used in genomic analysis and functional gene identification to help in the comprehensive understanding of the host's genetic response to stress factors and the molecular mechanisms of antioxidant defense systems.

The green peach aphid *Myzus persicae* (Sulzer) (Homoptera: Aphididae) is a worldwide pest that seriously harms >400 plants such as tobacco, cruciferous vegetables, peppers, and melons. This pest can cause the leaves of plants to curl, wither, and even die, thereby reducing crop yields (Weber 1985, Berlandier 2000). It can also spread >100 plant viruses as a viral vector and cause sooty blotch and mold parasitic infection through the secretion of honeydew, causing great losses in the production of cash crops (Berlandier 2000). *Myzus persicae* lives under direct sunlight throughout the year, so it cannot escape UV-B stress from the environment. However, the overall response mechanism of *M. persicae* to UV-B stress remains unclear at present. In this study, we performed a transcriptome sequencing analysis on the Illumina sequencing platform to ascertain the whole-genome transcriptional response of *M. persicae* under environmental UV-B stress. The results further clarified the antioxidant mechanisms of *M. persicae* and explored the molecular mechanisms of insect adaptation to UV-B environmental stress, providing novel targets for the prevention and management of pests.

Materials and Methods

Insects Rearing

Myzus persicae was raised in chambers at a temperature of 25°C ± 1°C and relative humidity of 70–80% under a 14-h/10-h photoperiod, in Institute of Entomology of Guizhou University.

UV-B Treatment

To exclude the influence of other light sources, *M. persicae* was fully dark adapted for 2 h, and then were divided into two groups: UV-B radiation and control groups (3 replicates per group, 30 aphids per replicate). In the first group, specimens were irradiated with UV-B

(280–320 nm) for 30 min at an intensity of 300 μW/cm². In the second group, specimens were irradiated using light-emitting diode fluorescent lamp bulbs for 30 min at the same intensity. The temperature and humidity during irradiation were consistent with the normal feeding conditions. Immediately after the end of treatment, insects were quickly frozen in liquid nitrogen and stored at –80°C until RNA was extracted.

RNA Isolation, Library Construction, and RNA Sequencing (RNA-seq)

Total RNA in *M. persicae* was extracted using TRIzol according to the manufacturer's instructions (Invitrogen), and genomic DNA was removed using DNase I (TaKaRa). The RNA quality was determined using a 2100 Bioanalyzer (Agilent) and quantified using a ND-2000 (NanoDrop Technologies). The sequence library was constructed using only high-quality RNA samples (OD260/280 = 1.8–2.2, OD260/230 ≥ 2.0, RIN ≥ 6.5, 28S:18S ≥ 1.0, >10 μg).

The RNA-seq transcriptome library was constructed using a TruSeq RNA sample preparation kit (Illumina, San Diego, CA). Poly-A mRNA was first enriched from 5 μg of total RNA using magnetic beads with oligo (dT). Then, fragmentation buffer was added to randomly degrade the mRNA into small fragments of approximately 200 bp. Next, double-stranded cDNA synthesis was performed with mRNA as a template using a SuperScript Double-Stranded cDNA Synthesis Kit (Invitrogen, CA) and a random hexamer primer (Illumina). The double-stranded cDNA structure was blunt-ended by adding End-Repair Mix (Enzymatics, USA), followed by addition of an 'A' base at the 3' end to ligate the Y-shaped link. The specific procedure is described in the specification. After amplifying cDNA via 15 cycles of PCR, a 200–300 bp target band was recovered using 2% agarose gel. After quantification using TBS380 (Picogreen), the library was subjected to high-throughput sequencing using the Illumina HiSeq 4000 sequencing platform with a sequencing read length of 2 × 150 bp.

Sequence Assembly

Quality control of raw data was achieved via sequencing using SeqPrep (<https://github.com/jstjohn/SeqPrep>) and Sickle (<https://github.com/najoshi/sickle>) with the default parameters (removing null reads, low-quality fragments, and an unknown base pair N sequence) to obtain a pure sequence. Afterwards, clean reads were separately aligned to the *M. persicae* reference genome for assembly using TopHat software (<http://tophat.cbcb.umd.edu/>, version 2.0.0) (Trapnell et al. 2009).

Differential Expression Analysis and Functional Enrichment

To identify differentially expressed genes (DEGs) between two different samples, fragments per kilobase of transcript per million mapped reads (FPKM) were used to quantify gene expression, and the count of reads was further normalized to the FPKM values. The corresponding significance thresholds for fold change (FC) and *P*-value were estimated using standardized gene expression levels (determined by the control false discovery rate [FDR]). Based on the expression level, the significance thresholds for DEGs in this study were FDR < 0.05 and FC > 1.5. In addition, the enrichment of DEGs was analyzed using Gene Ontology (GO) and Kyoto Encyclopedia of Genes and Genomes (KEGG). GO functional enrichment and KEGG pathway analyses were performed using Goatools (<https://github.com/tanghaibao/Goatools>) and KOBAS 2.0 (<http://kobas.cbi.pku.edu.cn/home.do>) (Xie et al. 2011).

qRT-PCR Verification

The 15 annotated unigenes were randomly selected for verification via qRT-PCR. Total RNA was extracted from specimens from each treatment group using TRIzol. The primers used for qRT-PCR are shown in [Supp Table S2 \(online only\)](#). cDNA was synthesized using a reverse transcription PrimeScript RT reagent kit (TaKaRa). qRT-PCR was performed on a C1000 real-time PCR system (Bio-Rad). In total, the 20 µl reaction mixture comprised 1 µl of cDNA (400 ng/µl), 10 µl of LYBR Green Supermix (TaKaRa), 1 µl of each of the primers (10 µmol/L), and 7 µl of ddH₂O. The *Glyceraldehyde-3-phosphate dehydrogenase* (*GAPDH*) and β -*actin* were used as internal reference genes ([Meng et al. 2019](#)). The 2^{- $\Delta\Delta$ Ct} method was used to analyze the relative differences in transcription levels ([Livak and Schmittgen 2001](#)). The geometric mean of two selected internal control genes was used for normalization, and experiments were performed using three biological replicates.

Results

mRNA Sequencing, Sequence Assembly, and Functional Annotation

In total, 177,070,180 (26.56 Gb) raw reads were generated from the two libraries (control and UV-B radiation groups) using Illumina HiSeq 4000 sequencing technology, and 7.81–8.02 million and 7.98–9.06 million clean reads were obtained from the two groups, respectively, after quality control decontamination ([Table 1](#)). The data quality of the clean reads for the control and UV-B radiation groups were separately evaluated. The results illustrated that the Q30 quality score exceeded 92% for both groups. The GC contents of the two groups were 41.16%–41.96% and 40.65%–41.50%, respectively, and >93% of the clean reads were independently aligned on the *M. persicae* reference genome, and <4% of the clean reads of both groups had multiple alignment positions on the reference genome. In addition, the intron region, 5' UTR, 3' UTR, and CDS comprised 1.62–1.90%, 6.10–6.96%, 3.96–4.70%, and 83.72–83.98% of the reads in the control group, respectively, versus 2.01–2.20%, 6.58–7.03%, 4.40–4.99%, and 82.57–83.48%, respectively, in the UV-B radiation group. These clean reads were assembled to obtain 40,699 unigenes, and the length distribution of all unigenes is shown in [Supp Fig. S1 \(online only\)](#). These results demonstrated that the sequencing quality was relatively high, indicating

that the unigenes were suitable for subsequent annotation analysis. We then annotated our unigenes using six functional databases and found that 37,226 (91.47%), 25,478 (62.60%), 29,164 (71.66%), 5,366 (13.18%), 16,885 (41.49%), and 18,898 (46.43%) unigenes could be mapped to the NR, Swiss-prot, Pfam, COG, GO, and KEGG databases, respectively.

Transcript Expression Analysis

To better classify the genes with different expression levels, genes were divided into three groups based on the FPKM value: high (FPKM > 10), medium (1 < FPKM ≤ 10), and low (0 < FPKM ≤ 1) ([Table 2](#)). The two libraries (control and UV-B radiation groups) included 7,058 and 6,611 genes with high expression, respectively ([Table 2](#)). UV-B stress had great influence on gene expression in *M. persicae*. Differential expression analysis identified 758 DEGs in the UV-B radiation group (423 upregulated, 335 downregulated) compared with their levels in the control group ([Supp Fig. S2 \(online only\)](#), [Supp Table S1 \(online only\)](#)).

GO and KEGG Analyses of DEGs

We focused on 423 upregulated and 335 downregulated genes to further understand the biological mechanism by which *M. persicae* responds to UV-B stress. In GO analysis, we grouped DEGs into three categories, namely, biological process, cellular component, and molecular function ([Fig. 1](#) and [Supp Table S3 \(online only\)](#)). In the biochemical process category, 'metabolic process', 'cell process', and 'single biological process' were significantly enriched. In the cell component category, 'membrane', 'cell part', 'membrane part', and 'cell' were significantly enriched. In the molecular function category, 'catalytic activity' and 'binding' were significantly enriched. In addition we also found that 31 DEGs were significantly associated with the 'response to stimulus'.

KEGG is a bioinformatics database for the systematic analysis of gene function ([Ogata et al. 1999](#)). In this study, 576 DEGs were annotated into 194 pathways, which were further divided into six categories as follows: cellular processes, environmental information processing, genetic information processing, metabolism, organismal systems, and human metabolism diseases ([Supp Table S4 \(online only\)](#)). The first 62 KEGG pathways are shown in [Fig. 2](#). Among these pathways, the immune and antioxidant defense, transport and catabolic, and signal transduction pathways were mainly enriched.

Table 1. Statistical analysis of transcriptome sequencing data

Samples	Control 1	Control 2	Control 3	UV-B 1	UV-B 2	UV-B 3
Clean reads	80,281,002	79,679,132	78,171,846	85,557,842	90,660,496	79,898,920
Clean bases	11,790,769,793	11,686,918,006	11,473,428,459	12,541,023,350	13,279,045,152	11,703,151,778
Q30 of clean reads	93.17%	92.87%	92.95%	92.74%	92.53%	92.63%
GC count	41.16%	41.26%	41.96%	41.38%	41.50%	40.65%
Total mapped reads	77,563,631	77,005,414	75,448,891	82,925,526	87,925,513	77,299,119
Multiple mapped reads	2,521,212 (3.14%)	1,944,693 (2.44%)	2,261,565 (2.89%)	2,128,105 (2.49%)	2,506,308 (2.76%)	1,787,924 (2.24%)
Uniquely mapped reads	75,042,419 (93.47%)	75,060,721 (94.20%)	73,187,326 (93.62%)	80,797,421 (94.44%)	85,419,205 (94.22%)	75,511,195 (94.51%)
Introns	1,949,073 (1.62%)	2,184,634 (1.84%)	2,207,153 (1.90%)	2,617,995 (2.07%)	2,702,377 (2.01%)	2,561,513 (2.20%)
3'UTR	5,647,225 (4.70%)	4,994,482 (4.21%)	4,590,588 (3.96%)	5,805,437 (4.60%)	5,904,505 (4.40%)	5,826,200 (4.99%)
5'UTR	7,317,961 (6.10%)	7,852,936 (6.62%)	8,065,925 (6.96%)	8,483,644 (6.72%)	9,438,718 (7.03%)	7,674,166 (6.58%)
CDS	100,508,905 (83.72)	99,602,642 (83.98%)	97,199,127 (83.88%)	105,067,869 (83.27%)	112,142,662 (83.48%)	96,351,330 (82.57%)

DEGs Involved in Antioxidant and Detoxification

In this study, we identified several genes involved in the regulation of antioxidant and detoxification mechanisms (Fig. 3). Seven DEGs in the peroxisome pathway were associated with antioxidant systems (del Río et al. 2002). In this pathway, fatty acyl-CoA reductase (Unigene15357 and Unigene11089), hydroxymethylglutaryl-CoA lyase (Unigene5738), mpv17-like protein 2 (Unigene7104), and long-chain-fatty-acid-CoA ligase five genes (Unigene9666) were upregulated, and two fatty acyl-CoA reductase genes (Unigene7287 and Unigene7290) were downregulated. In addition, we identified DEGs associated with metabolic detoxification, including genes encoding glutathione S-transferase (up: MSTRG.2702; down:

Unigene11295, Unigene1210, and MSTRG.2676), carboxylesterase (upregulated: Unigene9292, Unigene16134, Unigene7342, Unigene9915, Unigene10148, and Unigene6271; downregulated: Unigene6278), aldehyde dehydrogenase (Unigene1926), cytochrome P450 (CYP), and UDP-glucuronosyl transferase (UGT).

Metabolic and Protein Turnover

In this study, many metabolic reactions were significantly enhanced under UV-B stress in *M. persicae*, including carbohydrate (12 pathways), lipid metabolism (13 pathways), cofactor and vitamin metabolism (6 pathways), and amino acid metabolism (12 pathways) (Supp Table S5 [online only]). Among them, genes induced in carbohydrate metabolism included those involved in pyruvate metabolism (three DEGs), tricarboxylic acid cycle (TCA cycle) (three DEGs), glycolysis/gluconeogenesis (two DEGs), ascorbic acid and metabolism (four DEGs), and starch and sucrose metabolism (five DEGs). Moreover, we found that some genes related to amino acid metabolism were induced, including those involved in alanine, aspartate, and glutamate metabolism (three DEGs); glycine, serine, and threonine metabolism (two DEGs); cysteine and methionine (two DEGs); valine, leucine, and isoleucine degradation (seven DEGs); lysine degradation (three DEGs); and arginine and proline metabolism (one DEG).

Table 2. RNA sequencing results for gene expression in the two groups

Category	Control	UV-B
Highly expressed genes	7,058	6,611
Medium expressed genes	3,455	3,764
Low expressed genes	3,724	4,073
Total expressed genes	14,237	14,448
Unexpressed genes	3,258	2,772

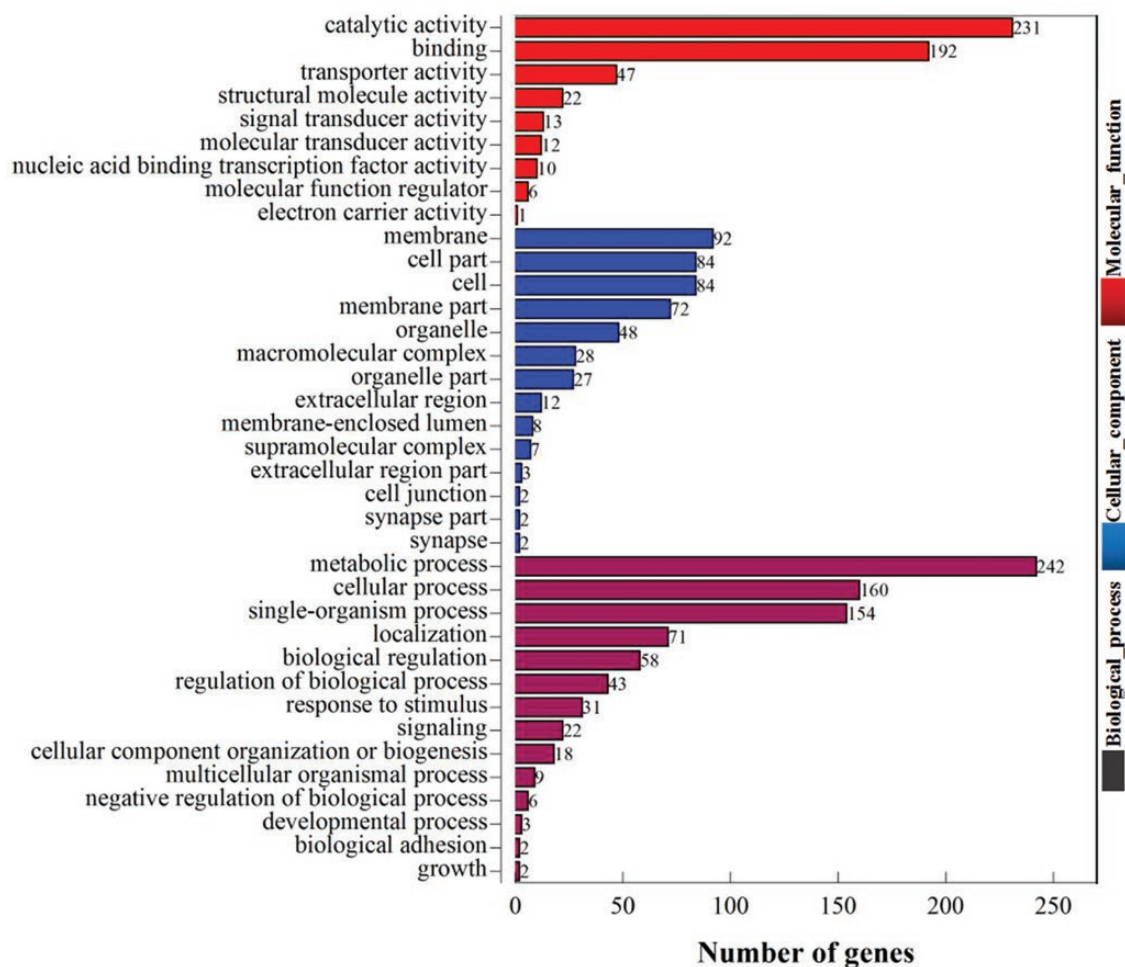


Fig. 1. Gene ontology enrichment of DEGs in *Myzus persicae* transcriptome under ultraviolet-B stress. All DEGs were grouped into three categories: biological process, cellular component, and molecular function.

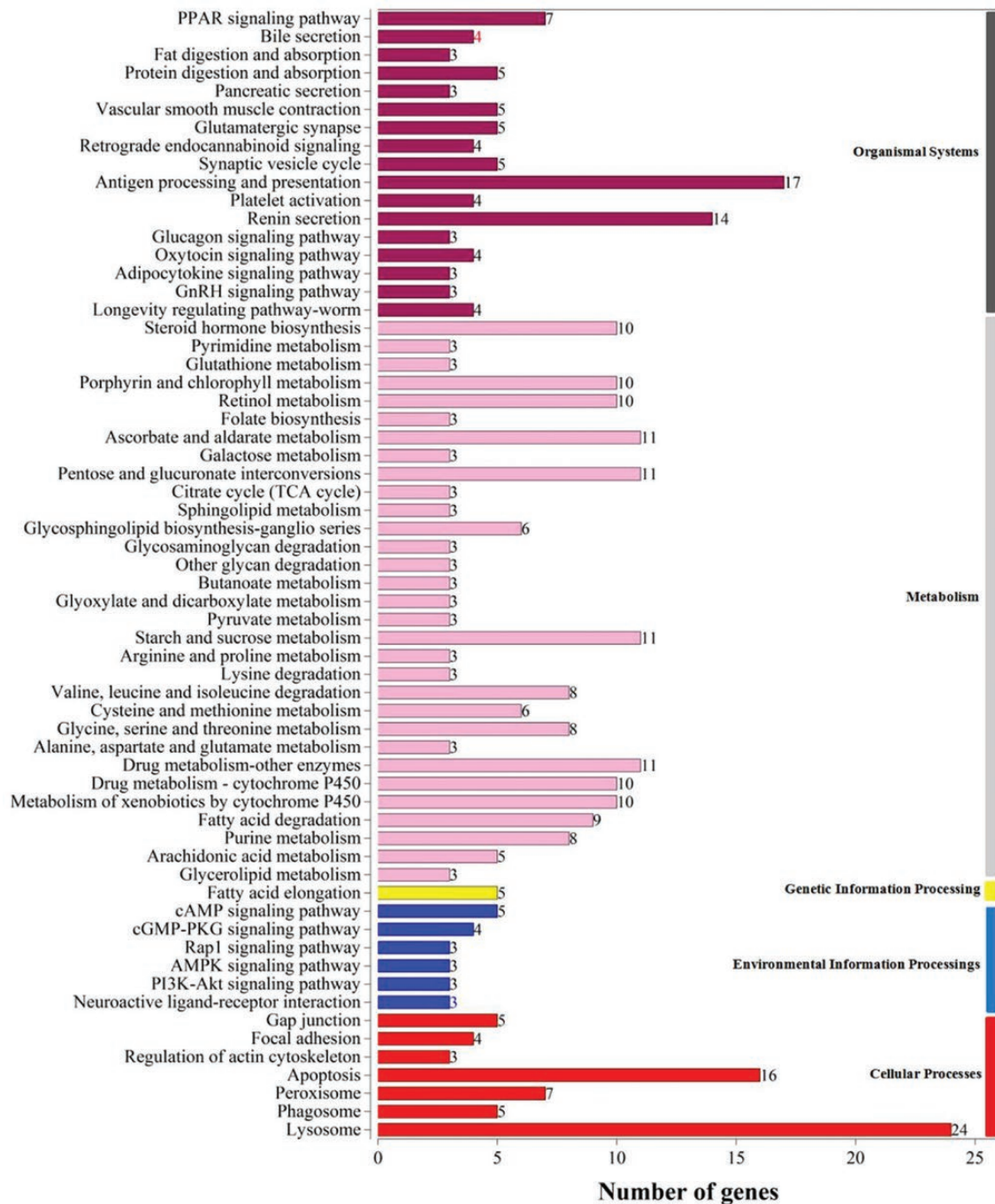


Fig. 2. KEGG classification analysis of differentially expressed genes Top 62 pathways according to enrichment factor as shown. The vertical axis presents the enriched KEGG pathways, and the horizontal

Immune Response

In our study, many immune-related DEGs were significantly enriched, most of which were upregulated in response to UV-B stress. These genes were mainly involved in five pathways, including antigen processing and presentation (17 DEGs), platelet activation (6 DEGs), and chemokine signaling pathways (3 DEGs) (Fig. 4). Nine, five, and two unigenes related to antigen processing and presentation, platelet activation, and chemokine signaling pathways, respectively, were upregulated. Among these, cathepsin B (CTSB) has 14 DEGs (6 upregulated and 8 downregulated) involved in the antigen processing and presentation pathways. In addition, some

antiviral genes such as serine proteinase inhibitor 2 (Unigene7537) and scavenger receptor class B (Unigene10115) genes were induced. Fc gamma R-mediated phagocytosis (Unigene7353) gene, which is involved in insect immunity, was upregulated.

Stress Signal Transduction

Many pathways involved in stress signal transduction were identified in our analysis, including PI3K-Akt (three DEGs), AMPK (three DEGs), Ras (two DEGs), Rap1 (three DEGs), calcium (two DEGs), cGMP-PKG (four DEGs), cAMP (five DEGs), and HIF-1 signaling pathways (two DEGs) (Supp Table S6 [online only]).

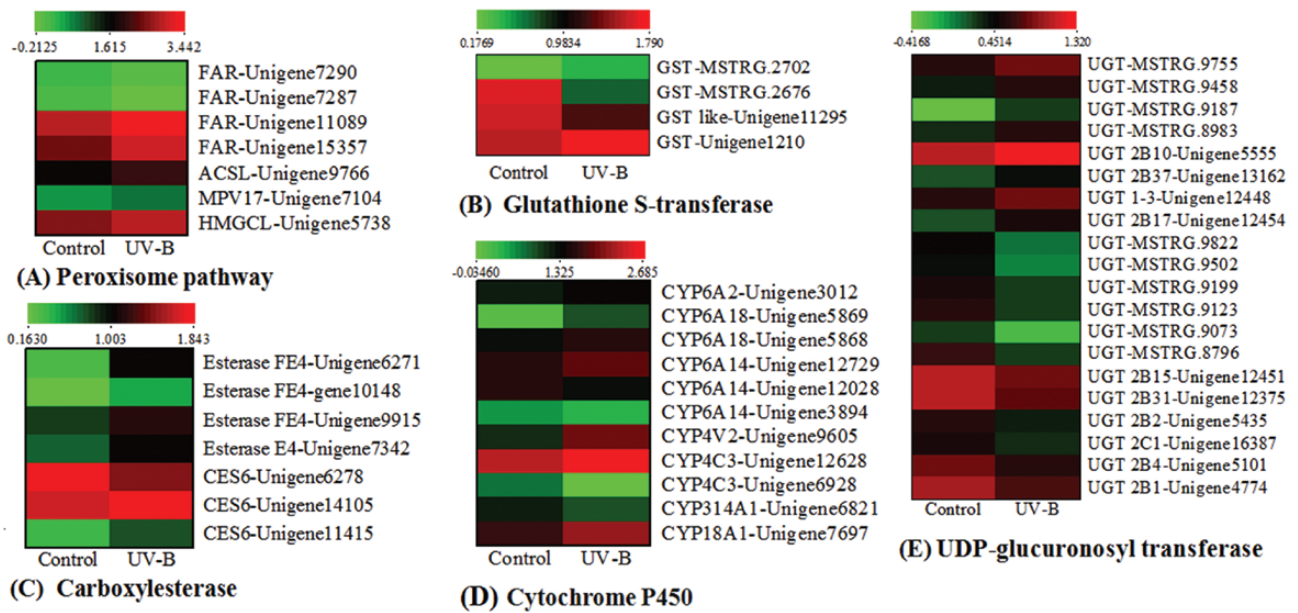


Fig. 3. Heatmap of antioxidant and detoxification gene expression under ultraviolet-B radiation. The expression levels of peroxisome pathway, glutathione S-transferase, carboxylesterase, cytochrome P450, and UDP-glucuronosyl transferase genes are presented in A, B, C, D, and E, respectively. The color scale is shown at the upper left, spanning from the lowest (green) to the highest (red) log₁₀ (expression) value.

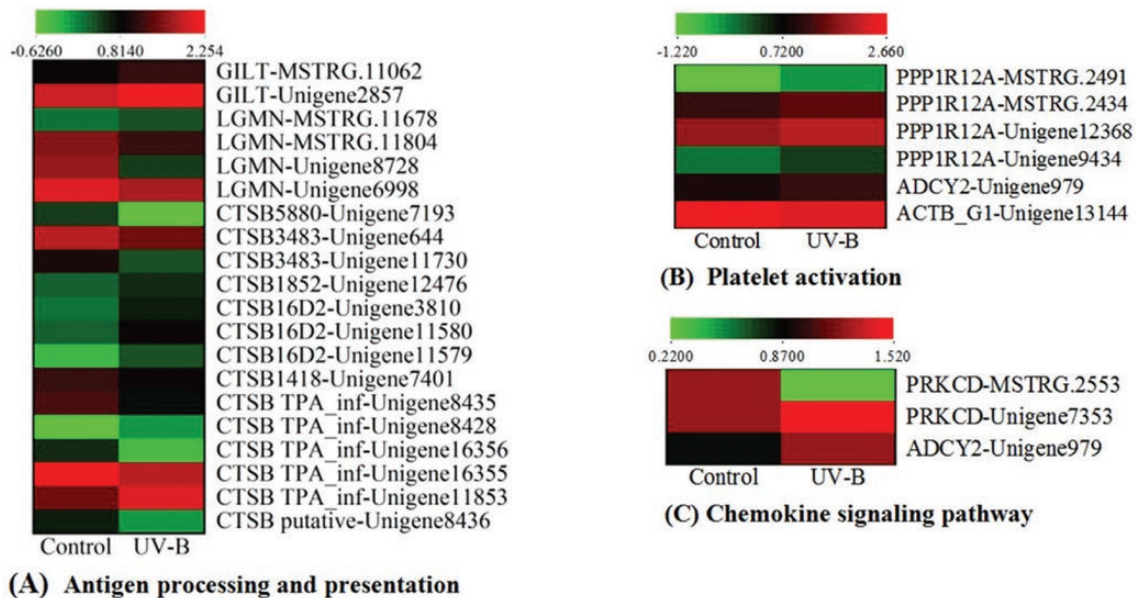


Fig. 4. Heatmap of immune response gene expression under UV-B radiation. The antigen processing and presentation, platelet activation, and chemokine signaling pathways are shown in A, B, and C, respectively. The color scale is shown at the upper left, spanning from the lowest (green) to the highest (red) log₁₀ (expression) value.

Validation of Expression Profiles Via qRT-PCR

To verify the transcriptome data, we randomly selected 15 genes and further tested their relative expression levels via qRT-PCR. According to comparative analysis, the trend of qRT-PCR results was consistent with the results of DEG expression analysis (Fig. 5), which verified the accuracy and reliability of the sequencing data.

Discussion

Most insects grow and multiply under direct sunlight and thus cannot escape the UV-B effect of direct sunlight. However, many insects also develop a variety of mechanisms, including morphological

and physiological adaptations, in response to UV-B stress. This may be due to the expression of certain unique genes in the body of insects. In this study, we performed a comparative transcriptional analysis of *M. persicae* to identify genes associated with the UV-B adaptability of this species. We identified 758 DEGs under UV-B stress (423 upregulated and 335 downregulated) and analyzed numerous biomarkers for antioxidants and detoxification, metabolic and protein turnover, immune response, and stress signal transduction. In GO analysis, 31 DEGs were significantly associated with the 'response to stimulus', which is related to the response of *M. persicae* to UV-B stress. Similar results have been reported for response of *Glyphodes pyloalis* to heat stress and the response of

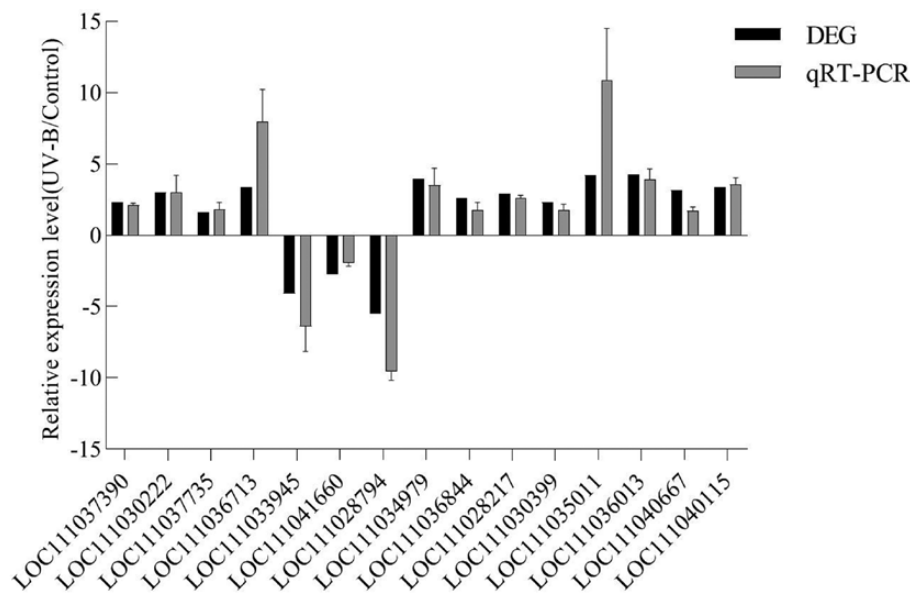


Fig. 5. qRT-PCR validation of DEGs in *M. persicae* under ultraviolet-B stress. DEGs were identified via RNA sequencing. The X-axis presents different unigenes. The Y-axis presents the relative expression levels of genes. *Glyceraldehyde-3-phosphate dehydrogenase* and β -actin were used as internal controls.

Antheraea pernyi to zinc stress (Liu et al. 2017, Liu et al. 2018). In addition, 92 DEGs were associated with ‘membrane’, suggesting that most cells of *M. persicae* need to be repaired under UV-B stress (Howard et al. 2011).

UV can result in ROS accumulation in insect cells, and the imbalance between ROS production and antioxidation can directly lead to a variety of toxic effects, including nonspecific DNA, protein, and lipid damage (Pitzschke et al. 2006, Meng et al. 2009, Gill and Tuteja 2010, Wang et al. 2012, Guo et al. 2019, Zhao et al. 2019). Several antioxidant-related genes, fatty acyl-CoA reductase (Unigene15357 and Unigene11089), hydroxymethylglutaryl-CoA lyase (Unigene5738), mpv17-like protein 2 (Unigene7104), and long-chain-fatty-acid-CoA ligase were significantly upregulated after UV-B treatment. These upregulated genes function as antioxidants to remove ROS in *M. persicae*. In addition, UV-B stress promotes the accumulation of toxic substances in *M. persicae*. Regarding detoxification and antioxidative mechanisms, glutathione S-transferase can catalyze the binding of the electrophilic group of endogenous harmful substances produced by UV-B stress to the thiol group of reduced glutathione, thereby forming a more soluble, nontoxic derivative that is easily excreted or decomposed by metabolic enzymes (Coleman et al. 1997). The activity of glutathione S-transferase in *Helicoverpa armigera* adults and *T. castaneum* were also significantly increased under UV stress (Meng et al. 2009, Guo et al. 2019). As an important serine hydrolase in insects, carboxylesterase can effectively catalyze the hydrolysis of various endogenous and exogenous compounds containing carboxyl ester bonds, amide bonds, and thioester bonds (Karunaratne et al. 1995). In our study, the expression levels of multiple carboxylesterase genes were significantly induced, which may help hydrolyze the harmful substances produced by UV-B exposure in the body of *M. persicae* (Jackson et al. 2013). The P450 and UGT enzyme system can metabolize various harmful endogenous and exogenous substances to protect living cells (Meech and Mackenzie 1997, Feyereisen 2011). However, under UV-B stress in *M. persicae*, unique eleven CYP and twenty UGT genes were induced, and these CYP genes were grouped into the six CYP6, three CYP4, one CYP314A1 (Shd), and one CYP18A1. *CYP6BQ4* and *CYP6BQ8* mRNA levels were also

significantly increased under UV-A stress in *T. castaneum* (Sang et al. 2012). The insect steroid hormone, 20-hydroxyecdysone (20E) controls and coordinates the development in insects, especially in the moulting/metamorphosis process of insect growth and development. To date, Halloween genes, namely *CYP307A1* (Spook, Spo)/*CYP307A2* (Spookier, Spok)/*CYP307B1* (Spookiest, Spot), *CYP306A1* (Phantom, Phm), *CYP302A1* (Disembodied, Dib), *CYP315A1* (Shadow, Sad), and *CYP314A1* (Shade, Shd), involved in the ecdysteroid biosynthesis have been identified and characterized in insects. The product of shd mediates the last step of the conversion from E into 20E (Christiaens et al. 2010). In this study, we found that the expression level of *M. persicae* shd gene was significantly down-regulated under UV-B exposure. We speculate that the synthesis of 20E in *M. persicae* may be inhibited under UV-B exposure, and its specific regulation mechanism needs to be confirmed by further studies. In addition, we also found that multiple cuticle protein genes (Unigene6813, Unigene6810, Unigene13926, Unigene9938, Unigene9939, Unigene15797, and Unigene8721) related to the development of *M. persicae* were significantly down-regulated under UV-B stress (Shang et al. 2020). The exoskeleton of insects (cuticle) is an assembly of chitin and cuticle proteins (Charles 2010). These results further prove that UV-B exposure has a greater impact on the growth and development of *M. persicae*.

Metabolism in insects plays a key role in environmental stress tolerance as the balance of energy demand and supply is crucial for survival. Our results indicated that the metabolism of *M. persicae* was enhanced under UV-B stress. Some genes related to TCA cycle, glycolysis, and pyruvate metabolism were significantly upregulated in *M. persicae* under UV-B stress. However, the TCA cycle and glycolysis are two important pathways for ATP production in insects; they are crucial for ensuring the energy supply of *M. persicae* in response to UV-B stress. Our results were consistent with those previously reported for *Macrosiphum euphorbiae* under UV-B stress and *Drosophila melanogaster* under UV-A stress (Nguyen et al. 2009, Zhou et al. 2013). UV-B stress leads to the accumulation of pyruvate, which can effectively remove ROS, reduce protein carbonylation, and stabilize mitochondrial membrane potential; these findings are similar to those reported in fungi under UV stress (Aguirre et al. 2006, Zhang et al. 2018b). Previous studies have shown that the vitamin D levels

were changed under UV-B exposure in migratory locusts, house crickets, yellow mealworms, and black soldier fly larvae insects (Oonincx et al. 2018). Similarity, in our study, it was also found that the expression level of phosphoserine aminotransferase (Unigene14435), which is related to the vitamin B6 metabolism, was significantly down-regulated in *M. persicae* after UV-B exposure. It suggests that vitamin metabolism is involved in the adaptive mechanisms of *M. persicae* in response to UV-B stress.

Because insects lack adaptive immunity, they can only rely on innate immune reactions for defense; however, these reactions also cause immunological changes during the stress response (Theopold and Dushay 2007, Adamo 2012). CTSB is an important proteolytic enzyme in insect lysosomes, which plays an important role in growth and metabolism by degrading protein activity and maintaining normal programmed cell death. As an important digestive protease present in various oviparous animals, CTSB provides nutrients for embryonic development by breaking down vitellin containing abundant amino acid components in the egg (Yamamoto et al. 1994, Matsumoto et al. 1997, Cho et al. 1999, Zhao et al. 2003, Zhao et al. 2005). Simultaneously, antiviral and FcγR-mediated phagocytosis of immune-related genes was induced under UV-B stress. These upregulated genes associated with immune responses indicate that many immune responses in insects can be activated under UV-B stress, illuminating the strong immune adaptive functions of insects (Adamo 2012, Adamo 2017).

The sensing and transduction of intracellular stress signals are critical for the adaptation and survival of insects following exposure to UV-B radiation. Studies indicated that the PI3K-Akt pathway activates the nuclear factor erythroid 2-related factor 2 pathway, which is a key factor that protects cells against damage induced by UV-B by inhibiting oxidative stress (Zhang et al. 2018a). Therefore, activation of the PI3K-Akt pathway may be critical in the insect response to UV-B stress. As an important pressure-sensing and energy-regulating factor, AMPK is essential for the survival of organisms in harsh environments. Under UV-B stress, the AMPK signaling pathway in *M. persicae* was activated, and this activation is related to its molecular adaptation mechanism under UV-B stress (Zhu et al. 2007, Hardie 2011). Activation of the cGMP-PKG signaling pathway mobilizes intracellular Zn²⁺ to prevent mitochondrial oxidative damage in cardiomyocytes (Jang et al. 2007). However, UV-B stress can cause significant ROS accumulation and damage to organisms. Activation of the cGMP-PKG signaling pathway can protect mitochondria in insect cells. These findings indicated that signal transduction plays an important role in the response of *M. persicae* to UV-B stress.

Conclusions

In summary, in this study, we used RNA-seq for the first time to narrate the genes associated with the adaptation of *M. persicae* to UV-B stress. The results illustrated that the adaptive mechanism of *M. persicae* to UV-B stress is complex, mainly involving genes involved in antioxidation, detoxification, metabolic and protein turnover, immune response, and stress signal transduction. Our results clarify the molecular mechanism underlying the adaptation of *M. persicae* to UV-B stress as well as provide a basis for us to further study the molecular mechanism of insects' adaptation to environmental factors such as UV-B stress.

Supplementary Data

Supplementary data are available at *Journal of Insect Science* online.

Figure S1. Length distribution of the unigenes in the *Myzus persicae* transcriptome.

Figure S2. Volcano plot of differentially expressed genes. The Y-axis presents $-\log_{10}$ significance. The X-axis presents \log_2 (fold change). Dots represent individual genes. Red dots represent upregulated genes, and blue dots denote downregulated genes. Black dots indicate genes that were not differentially expressed.

Acknowledgments

We thank Charlesworth Group (<https://www.researchsquare.com/article/rs-8935/v1>) for editing a draft of this manuscript. This manuscript has been released as a pre-print at research square (Yang et al. 2019). This research was supported by the National Natural Science Foundation of China (grant number 31460483), Guizhou Science Technology Foundation (J[2011]2135), Guizhou Tobacco Company Program (2021XM09, 201937), and the Guangdong Province Science and Technology Special Fund Project (2019A103009).

Author Contributions

Conceptualization, C.-L.Y. and C.-Y.Z.; Methodology, C.-L.Y. and C.-Y.Z.; Software, C.-L.Y., J.-Y.M., and M.-S.Y.; Validation, C.-L.Y. and M.-S.Y.; Formal Analysis, C.-L.Y. and J.-Y.M.; Investigation, C.-L.Y. and M.-S.Y.; Resources, C.-Y.Z.; Data Curation, C.-Y.Z.; Writing—Original Draft Preparation, C.-L.Y. and J.-Y.M.; Writing—Review and Editing, C.-L.Y., J.-Y.M., M.-S.Y., and C.-Y.Z. All authors have read and agreed to the published version of the manuscript.

Data Availability

RNA sequencing raw data have been deposited in the NCBI Sequence Read Archive (SRA; accession number PRJNA592018).

References Cited

- Adamo, S. A. 2012. The effects of the stress response on immune function in invertebrates: an evolutionary perspective on an ancient connection. *Horm. Behav.* 62: 324–330.
- Adamo, S. A. 2017. Stress responses sculpt the insect immune system, optimizing defense in an ever-changing world. *Dev. Comp. Immunol.* 66: 24–32.
- Aguirre, J., W. Hansberg, and R. Navarro. 2006. Fungal responses to reactive oxygen species. *Med. Mycol.* 44: S101–S107.
- Berlandier, F. A. 2000. Aphids on the world's crops. An information and identification guide. *Austral Entomol.* 39: 354–355.
- Bode, H. B. 2009. Insects: true pioneers in anti-infective therapy and what we can learn from them. *Angew. Chem. Int. Ed.* 48: 6394–6396.
- Charles, J. P. 2010. The regulation of expression of insect cuticle protein genes. *Insect Biochem. Mol. Biol.* 40: 205–213.
- Cho, W. L., S. M. Tsao, A. R. Hays, R. Walter, J. S. Chen, E. S. Snigirevskaya, and A. S. Raikhel. 1999. Mosquito cathepsin B-like protease involved in embryonic degradation of vitellin is produced as a latent extraovarian precursor. *J. Biol. Chem.* 274: 13311–13321.
- Christiaens, O., M. Iga, R. A. Velarde, P. Rougé, and G. Smaghe. 2010. Halloween genes and nuclear receptors in ecdysteroid biosynthesis and signalling in the pea aphid. *Insect Mol. Biol.* 19(Suppl 2): 187–200.
- Croucher, N. J., M. C. Fookes, T. T. Perkins, D. J. Turner, S. B. Marguerat, T. Keane, M. A. Quail, M. He, S. Assefa, J. Bähler, et al. 2009. A simple method for directional transcriptome sequencing using Illumina technology. *Nucleic Acids Res.* 37: e148.
- Coleman, J., M. Blake-Kalff, E. Davies. 1997. Detoxification of xenobiotics by plants: chemical modification and vacuolar compartmentation. *Trends Plant Sci.* 2: 144–151.
- Dahms, H. U., and J. S. Lee. 2010. UV radiation in marine ectotherms: molecular effects and responses. *Aquat. Toxicol.* 97: 3–14.
- Feyerisen, R. 2011. Arthropod CYPomes illustrate the tempo and mode in P450 evolution. *Biochim. Biophys. Acta.* 1814: 19–28.
- Gill, S. S., and N. Tuteja. 2010. Reactive oxygen species and antioxidant machinery in abiotic stress tolerance in crop plants. *Plant Physiol. Biochem.* 48: 909–930.

- Guo, S. H., L. Yu, Y. M. Liu, F. F. Wang, Y. C. Chen, Y. Wang, B. L. Qiu, W. Sang. 2019. Digital gene expression profiling in larvae of *Tribolium castaneum* at different periods post UV-B exposure. *Ecotox. Environ. Safe.* 174: 514–523.
- Hardie, D. G. 2011. AMP-activated protein kinase—an energy sensor that regulates all aspects of cell function. *Gene. Dev.* 25 (18): 1895–1908.
- Hideg, É., M. A. K. Jansen, A. Strid. 2013. UV-B exposure, ROS, and stress: inseparable companions or loosely linked associates? *Trends Plant Sci.* 18: 107–115.
- Hu, Z. Q., H. Y. Zhao, and T. Thieme. 2013. The effects of enhanced ultraviolet-B radiation on the biology of green and brown morphs of *Sitobion avenae* (Hemiptera: Aphididae). *Environ. Entomol.* 42: 578–585.
- Jackson C. J., J. W. Liu, P. D. Carr, F. Younus, C. Coppin, T. Meirelles, M. Lethier, G. Pandey, D. L. Ollis, R. J. Russell, M. Weik, J. G. Oakeshott. 2013. Structure and function of an insect α -carboxylesterase (Esterase7) associated with insecticide resistance. *Proc. Natl. Acad. Sci. USA* 110: 10177–10182.
- Jang, Y., H. Wang, J. Xi, R. A. Mueller, E. A. Norfleet, and Z. Xu. 2007. NO mobilizes intracellular Zn²⁺ via cGMP/PKG signaling pathway and prevents mitochondrial oxidant damage in cardiomyocytes. *Cardiovasc. Res.* 75: 426–433.
- Karunaratne, S. H., J. Hemingway, K. G. Jayawardena, V. Dassanayaka, and A. Vaughan. 1995. Kinetic and molecular differences in the amplified and non-amplified esterases from insecticide-resistant and susceptible *Culex quinquefasciatus* mosquitoes. *J. Biol. Chem.* 270: 31124–31128.
- Karthi, S., R. Sankari, and M. S. Shivakumar. 2014. Ultraviolet-B light induced oxidative stress: effects on antioxidant response of *Spodoptera litura*. *J. Photochem. Photobiol. B.* 135: 1–6.
- Lidon, F. J. C., M. Teixeira, J. C. Ramalho. 2012. Decay of the chloroplast pool of ascorbate switches on the oxidative burst in UV-B-irradiated rice. *J. Agron. Crop Sci.* 198: 130–44.
- Liu, Y., H. Su, R. Li, X. Li, Y. Xu, X. Dai, Y. Zhou, and H. Wang. 2017. Comparative transcriptome analysis of *Glyphodes pyloalis* Walker (Lepidoptera: Pyralidae) reveals novel insights into heat stress tolerance in insects. *BMC Genomics.* 18: 974.
- Liu, Y., Z. Z. Xin, J. Song, X. Y. Zhu, Q. N. Liu, D. Z. Zhang, B. P. Tang, C. L. Zhou, and L. S. Dai. 2018. Transcriptome analysis reveals potential antioxidant defense mechanisms in *Antheraea pernyi* in response to zinc stress. *J. Agric. Food Chem.* 66: 8132–8141.
- Livak, K. J., and T. D. Schmittgen. 2001. Analysis of relative gene expression data using real-time quantitative PCR and the 2^{(-Delta Delta C(T))} Method. *Methods.* 25: 402–408.
- Matsumoto, I., Y. Emori, K. Abe, and S. Arai. 1997. Characterization of a gene family encoding cysteine proteinases of *Sitophilus zeamais* (Maize Weevil), and analysis of the protein distribution in various tissues including alimentary tract and germ cells. *J. Biochem.* 121: 464–476.
- McKenzie, R. L., P. J. Aucamp, A. F. Bais, L. O. Björn, and M. Ilyas. 2007. Changes in biologically-active ultraviolet radiation reaching the Earth's surface. *Photochem. Photobiol. Sci.* 6: 218–231.
- Meech, R., P. I. Mackenzie. 1997. Structure and function of uridine diphosphate glucuronosyl transferases. *Clin. Exp. Pharmacol P.* 24: 907–915.
- Meng, J. Y., C. Y. Zhang, F. Zhu, X. P. Wang, and C. L. Lei. 2009. Ultraviolet light-induced oxidative stress: effects on antioxidant response of *Helicoverpa armigera* adults. *J. Insect Physiol.* 55: 588–592.
- Meng, J., X. Chen, and C. Zhang. 2019. Transcriptome-based identification and characterization of genes responding to imidacloprid in *Myzus persicae*. *Sci. Rep.* 9: 13285.
- Nguyen, T. T., D. Michaud, and C. Cloutier. 2009. A proteomic analysis of the aphid *Macrosiphum euphorbiae* under heat and radiation stress. *Insect Biochem. Mol. Biol.* 39: 20–30.
- Ogata, H., S. Goto, K. Sato, W. Fujibuchi, H. Bono, and M. Kanehisa. 1999. KEGG: Kyoto Encyclopedia of Genes and Genomes. *Nucleic Acids Res.* 27: 29–34.
- Oonincx, D. G. A. B., P. van Keulen, M. D. Finke, F. M. Baines, M. Vermeulen, and G. Bosch. 2018. Evidence of vitamin D synthesis in insects exposed to UVb light. *Sci. Rep.* 8: 10807.
- Paul, N., D. Gwynn-Jones. 2003. Ecological roles of solar UV radiation: towards an integrated approach. *Trends Ecol. Evol.* 18: 48–55.
- Pitzschke, A., C. Forzani, and H. Hirt. 2006. Reactive oxygen species signaling in plants. *Antioxid. Redox Signal.* 8: 1757–1764.
- Potter, K. A., H. A. Woods. 2013. Immobile and tough versus mobile and weak: effects of ultraviolet B radiation on eggs and larvae of *Manduca sexta*. *Physiol. Entomol.* 38: 246–252.
- del Río, L. A., F. J. Corpas, L. M. Sandalio, J. M. Palma, M. Gómez, and J. B. Barroso. 2002. Reactive oxygen species, antioxidant systems and nitric oxide in peroxisomes. *J. Exp. Bot.* 53: 1255–1272.
- Rünger, T. M., and U. P. Kappes. 2008. Mechanisms of mutation formation with long-wave ultraviolet light (UVA). *Photodermatol. Photoimmunol. Photomed.* 24: 2–10.
- Sang, W., W. H. Ma, L. Qiu, Z. H. Zhu, and C. L. Lei. 2012. The involvement of heat shock protein and cytochrome P450 genes in response to UV-A exposure in the beetle *Tribolium castaneum*. *J. Insect Physiol.* 58: 830–836.
- Sang, W., L. Yu, L. He, W. H. Ma, Z. H. Zhu, F. Zhu, X. P. Wang, and C. L. Lei. 2016. UVB radiation delays *Tribolium castaneum* metamorphosis by influencing ecdysteroid metabolism. *PLoS One.* 11: e0151831.
- Shang, F., B. Y. Ding, C. Ye, L. Yang, T. Y. Chang, J. Xie, L. D. Tang, J. Niu, and J. J. Wang. 2020. Evaluation of a cuticle protein gene as a potential RNAi target in aphids. *Pest Manag. Sci.* 76: 134–140.
- Theopold, U., M. Dushay. 2007. Mechanisms of *Drosophila* immunity—an innate immune system at work. *Curr. Immunol. Rev.* 3: 276–288.
- Trapnell, C., L. Pachter, and S. L. Salzberg. 2009. TopHat: discovering splice junctions with RNA-Seq. *Bioinformatics.* 25: 1105–1111.
- Vandenbussche, F., N. Yu, W. Li, L. Vanhaelewyn, M. Hamshou, D. Van Der Straeten, and G. Smaghe. 2018. An ultraviolet B condition that affects growth and defense in *Arabidopsis*. *Plant Sci.* 268: 54–63.
- Villena, O. C., B. Momen, J. Sullivan, and P. T. Leisnham. 2018. Effects of ultraviolet radiation on metabolic rate and fitness of *Aedes albopictus* and *Culex pipiens* mosquitoes. *Peerj.* 6: e6133.
- Wang, Y., L. Wang, Z. Zhu, W. Ma, and C. Lei. 2012. The molecular characterization of antioxidant enzyme genes in *Helicoverpa armigera* adults and their involvement in response to ultraviolet-A stress. *J. Insect Physiol.* 58: 1250–1258.
- Wasielowski, O., T. Wojciechowicz, K. Giejdasz, and N. Krishnan. 2015. Enhanced UV-B radiation during pupal stage reduce body mass and fat content, while increasing deformities, mortality and cell death in female adults of solitary bee *Osmia bicornis*. *Insect Sci.* 22: 512–520.
- Weber, G. 1985. Genetic variability in host plant adaptation of the green peach aphid, *Myzus persicae*. *Entomol. Exp. Appl.* 38: 49–56.
- Xie, C., X. Mao, J. Huang, Y. Ding, J. Wu, S. Dong, L. Kong, G. Gao, C. Y. Li, and L. Wei. 2011. KOBAS 2.0: a web server for annotation and identification of enriched pathways and diseases. *Nucleic Acids Res.* 39: W316–W322.
- Yamamoto, Y., X. F. Zhao, A. C. Suzuki, and S. Y. Takahashi. 1994. Cysteine proteinase from the eggs of the silkworm, *Bombyx mori*: site of synthesis and a suggested role in yolk protein degradation. *J. Insect Physiol.* 40: 447–454.
- Yang, C. L., C. Y. Zhang, J. Y. Meng, and M. S. Yao. 2019. Transcriptome analysis reveals the potential antioxidant defense mechanisms of *Myzus persicae* in response to UV-B stress. *Research Square*, 12 December, Preprint (<https://www.researchsquare.com/article/rs-8935/v1>).
- Zhang, B., Z. Zhao, X. Meng, H. Chen, G. Fu, and K. Xie. 2018a. Hydrogen ameliorates oxidative stress via PI3K-Akt signaling pathway in UVB-induced HaCaT cells. *Int. J. Mol. Med.* 41: 3653–3661.
- Zhang, X., R. J. St Leger, and W. Fang. 2018b. Stress-induced pyruvate accumulation contributes to cross protection in a fungus. *Environ. Microbiol.* 20: 1158–1169.
- Zhao, X. F., J. X. Wang, X. L. Xu, R. Schmid, H. Wiczorek. 2003. Molecular cloning and characterization of the cathepsin B-like proteinase from the cotton boll worm, *Helicoverpa armigera*. *Insect Mol. Biol.* 11 (6): 567–575.
- Zhao, X. F., X. M. An, J. X. Wang, D. J. Dong, X. J. Du, S. Sueda, and H. Kondo. 2005. Expression of the *Helicoverpa* cathepsin B-like proteinase during embryonic development. *Arch. Insect Biochem.* 58: 39–46.
- Zhao, C., J. Ding, M. Yang, D. Shi, D. Yin, F. Hu, J. Sun, X. Chi, L. Zhang, and Y. Chang. 2019. Transcriptomes reveal genes involved in covering and sheltering behaviors of the sea urchin *Strongylocentrotus intermedius* exposed to UV-B radiation. *Ecotoxicol. Environ. Saf.* 167: 236–241.
- Zhu, X. J., C. Z. Feng, Z. M. Dai, R. C. Zhang, and W. J. Yang. 2007. AMPK alpha subunit gene characterization in *Artemia* and expression during development and in response to stress. *Stress.* 10: 53–63.
- Zhou, L. J., Z. H. Zhu, Z. X. Liu, W. H. Ma, N. Desneux, and C. L. Lei. 2013. Identification and transcriptional profiling of differentially expressed genes associated with response to UVA radiation in *Drosophila melanogaster* (Diptera: Drosophilidae). *Environ. Entomol.* 42: 1110–1117.